The Evolution of Urbanization in Dodoma: A 21-Year Spatial Assessment

Neema S. Sumari

Department of Informatics and Information Technology, College of Natural and Applied Sciences (CoNAS), Sokoine University of Agriculture, P.O. Box 3038, Morogoro, Tanzania

Correspondence: neydsumari@gmail.com

Keywords: Urban Expansion Intensity Index; Landsat remote sensing; Shannon’s Entropy Index; Urban landscape change; Dodoma-Tanzania

Abstract:

This preliminary study investigates the rapid urbanization of Dodoma, the Capital City of the Republic of Tanzania, over 21 years (1997–2018). The rapid urbanization of cities worldwide is leading to significant changes in land use and land cover patterns, particularly in emerging urban centers. Monitoring the spatial and temporal dynamics of these changes is essential for effective urban planning and sustainable development. Using time-series Landsat satellite data, the study examines the spatial expansion of urban areas and the resulting changes to the landscape in Dodoma. The Urban Expansion Intensity Index (UEII) and Shannon’s Entropy Index (SEI) were applied to assess the extent and patterns of urban growth. The results indicate that Dodoma has undergone rapid urbanization, with the northern region showing an SEI of 0.439 and the southern region an SEI of 0.371 between 1997 and 2018. Additionally, Sorenson’s UEII coefficient reveals an urban growth rate of approximately 9,131 hectares over the same period, with a coefficient value of 0.224. These findings are significant for the achievement of Sustainable Development Goal 11 (SDG-11), which advocates for the development of sustainable cities and communities. The study emphasizes the need for comprehensive federal policies to monitor urban dynamics and safeguard ecological resources as Dodoma and other emerging cities across Tanzania continue to expand.

1. Introduction

Globally, the process of increasing urban dwellers is leading to rapid landscape changes in emerging urban cities. In 2018, for instance, about 26.5% of the world's inhabitants lived in cities with less than 0.5 million dwellers (Cobbinah & Darkwah, 2017; Xu, Dong, et al., 2019). Similarly, from 2018 to 2030, the number of cities with 0.5 million people or more was expected to increase by 23% in Asia and by 57% in Africa(Wu et al., 2021; Xiao et al., 2024). This scenario has a likelihood to cause fast urban expansion and amplify the stress on neighboring ecosystems. Thus, rapid population growth and the related need for housing and other amenities have resulted in an increasing urbanized land cover types in most African countries. Most physical developments in Africa are typically characterized by scattered spatially distributed infrastructures. Meanwhile, a congested spatial distribution of infrastructures is asserted that needs to be better for enhancing transportation system as well as minimizing the consumption of traffic energy-efficiency and resource utilization such as water pipe networks and drainage systems (Mwampamba, 2007; Pandey & Seto, 2015). Spatiotemporal analysis of urban expansion has been an enthusiastic question that has dominated over a long time of years, yet remains a concept major without a key definition or measurement (Lai et al., 2018).

Although several studies have focused on urban growth and expansion in various cities and regions in Tanzania, including Dar es Salaam, there is a notable lack of information on the spatiotemporal impact analysis of urban expansion on the vegetation landscape using remote sensing approaches in the Dodoma region. This gap is particularly significant in the context of contributing to sustainable cities in line with the United Nations Sustainable Development Goals. The term "spatiotemporal" is used in spatial data analysis when data is collected across both space and time. Studies by Lai et al. (2018) and Sumari et al., (2020), who conducted spatiotemporal analyses of urban growth using GIS and remote sensing approaches, concluded that urban growth in evolving regions is influenced by population growth driven by both natural increase and in-migration.

Urbanization is typically a spatial population process that indicates the significant role that towns and cities play in the population distribution of a given socioeconomic setup (Jiao et al., 2021; Korah & Cobbinah, 2017; Shao et al., 2021). This process typically occurs as a result of changes in population distribution from villages and the countryside, which were the origins of human society, to cities and urban residences. Urbanization, on the other hand, is viewed as a spatial and social process that results in a shift in the relationship between human societies and social behaviors across multiple dimensions. This process addresses the complex

transformations in human societies' lifestyles that have a direct impact on urban communities. The importance of spatial integration and the dynamism of urban growth cannot be overstated issues in urban studies today.

The overall objective of this study, therefore, is to assess the spatiotemporal impacts of urban expansion and landscape with a remote sensing approach in Dodoma Urban District (DUD) towards contributing to sustainable cities in line with the United Nations Sustainable Development Goals.

1.1 Spatiotemporal Analysis: A Literature Review

However, various studies have identified several consequences of congested urban areas, including the loss of urban green spaces, increased air pollution in African cities, and clustered services (Addaney & Cobbinah, 2019; Kontgis et al., 2014). Although there is some debate regarding spatial indices of urban growth types, there is general agreement that urban spatial morphology can promote the development of urban green spaces, which are considered important natural assets for reducing urban heat island effects and providing comfort to urban dwellers (Kabanda, 2019; Xiong et al., 2012). Based on these findings, understanding the implications and dynamics of rapid changes in urbanized landscapes, especially in emerging African cities, can help achieve sustainable cities, improve ecosystem services, and mitigate the impacts of climate change amid growing human populations. Consequently, the exploration of urban spatial dynamics and the analysis of urban landscape structures continue to be areas of interest for the sustainable cities research community.

Several scientific studies have investigated the impacts of urban expansion on landscape composition and configuration (Sumari et al., 2020; Xu, Dong, et al., 2019; Xu, Jiao, et al., 2019), including the examination of existing and projected urban land cover dynamics (Gombe et al., 2017; Yang, Pan, et al., 2017), as well as exploring the patterns and possible drivers of urban sprawl (Guastella et al., 2019). However, previous studies have primarily focused on large metropolitan regions due to their significant influence on socio-economic and environmental conditions (Cobbinah, 2015; Mundia & Murayama, 2009). In contrast, smaller cities and towns, where scattered urban growth is more prominent, have received relatively little attention (Jia et al., 2017; Terfa et al., 2019). Given that small cities are expected to dominate global urbanization in the future, it is crucial to study the spatial and temporal changes of these emerging smaller cities by combining urban landscape analysis with remote sensing techniques to evaluate the patterns of urban landscape structures.

By evaluating the urban landscape structures, on one hand, the landscape heterogeneity, and the impact of different ecological services associated with cities can be ascertained (Brusseau, 2019). Landscape metrics can be useful in revealing the general circumstances of the urban landscape pattern (Qin et al., 2017), triggers of urban land use, and change analysis (Lu et al., 2016; Xu, Zhou, et al., 2019), as well as assessing the projected future urban spatial form (Wang & Upreti, 2019; Worrall et al., 2017). Landscape metrics studies are also primarily applied to detect the relationship between landscape patterns and land surface temperature (Bonafoni & Keeratikasikorn, 2018; Fu et al., 2017).

On the other hand, remote sensing methods can complement the afore-explained landscape metrics approach in determining the temporal and spatial characteristics of urban land cover types towards addressing any unforeseeable and severe ecological concerns threatening urban populations (Meng et al., 2018). Remote sensing is a valuable tool for estimating infrastructural growth in urban areas. Remote sensing techniques have been tested to provide data at multiple spatial scales in urban areas, based on the processing and interpretation of satellite images (Kuffer et al., 2018). As such, open-source satellite remote sensing (RS) data have proven to be a cost-effective source of spatial information for all aspects of urban analyses. Optical satellite sensors of Landsat (30m spatial resolution) are probably the most popular sensors for land cover mapping in African urban areas because the data has relatively high temporal resolution and is freely available. Therefore, this present study focuses on assessments of urban expansion indices in the Federal Capital City of Dodoma in Tanzania using Landsat satellite data.

The urban growth in Dodoma, and likely in many other cities and towns across Tanzania, is generally characterized by a lack of implementation plans such as maps that often have a shortage of necessary infrastructure and services(Chove & Sumari, 2025; Kisamba & Li, 2023). The absence of urban planning plans could also contribute to fragmented urban landscape patterns along major roadways. Over the past couple of decades, regional cities in Tanzania have grown faster than the capital city, Dodoma Urban (Ringo, 2016). This feature can likely be explained by considering the national economic development and urban improvement policies (Yang, Wu, et al., 2017) that fostered rapid urban expansion in secondary and tertiary cities.

2. Methodology

2.1 Study Area

The study was focused in the central part of mainland Tanzania, Dodoma Urban District (DUD) (Figure 1). Dodoma region is the federal capital city of the county and it doubles as a regional state in Tanzania. The Government of Tanzania established The Capital Development Authority (CDA) in 1974 through Government Notice No. 230 of 12th October to move the capital from Dar Es Salaam to DUD (URT, 2018). Consequently, the seat of the federal government was officially from Dar Es Salaam to Dodoma region in 2016.

The region has several geographical features, including topographical areas with flatlands, gentle hills, and lowlands, some of which contain seasonal dams. The rainfall is primarily used for agricultural irrigation purposes. Dodoma also has wetlands and seasonal swamps(Kisamba & Li, 2023). The soil

in the region is generally shallow with moderate fertility, moderate organic matter content, and poor permeability, leading to higher surface runoff. Vegetation cover has been decreasing due to human activities, including agriculture, lumbering, bushfires, fuelwood and charcoal extraction, and grazing.

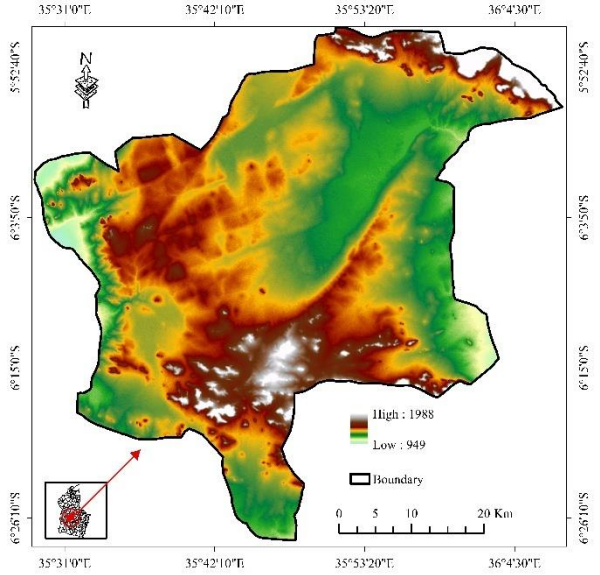

Figure 1: *Map of study area*

The geographical location of the Dodoma region lies between latitude 4°S and 7°S and longitude 35°E and 37°E. Administratively, the region is divided into seven districts: Bahi, Chemba, Chamwino, Dodoma Urban District (DUD), Kondoa, Kongwe, and Mpwapwa. It is bordered by four other regions: Morogoro to the east, Singida to the west, Arusha to the north, and Iringa to the south. According to the 2012 Population and Housing Census, the population of Dodoma Urban was 410,956, with 199,487 males and 211,469 females (URT, 2018). The region's population is growing rapidly due to increasing economic activities, such as trade and the establishment of higher learning institutions, which have triggered a massive influx of people into Dodoma Urban District (DUD). Current population projections estimate the population of Dodoma at approximately 414,906 (Ringo, 2016).

2.2 Description of Remote Sensing Data

Cloud-free images from three Landsat optical sensors—the Landsat Thematic Mapper (TM), the Landsat Enhanced Thematic Mapper Plus (ETM+), and the Landsat Operational Land Imager (OLI), also known as Landsat 8—were used in this study. The Landsat images were acquired for the years 1997 (TM), 2004 (ETM+), 2011 (ETM+), and 2018 (OLI). All images were obtained from the United States Geological Survey (USGS) website (http://earthexplorer.usgs.gov/) with path/row number 168/064. Image classification was performed using ENVI version 5.3, while accuracy assessments were carried out using ERDAS Imagine version 2014 and ArcGIS version 10.3 for image data processing, visualization, and map production.

2.3 Landcover Analysis in DUD

To assess urban expansion in this study, Landsat 5, Landsat 7, and Landsat 8 imagery from the years 1997, 2004, 2011, and 2018 were used to extract built-up areas. The land cover types in Dodoma were classified into two main categories: (1) built-up areas and (2) non-built-up areas. The non-built-up areas were further categorized into the northern and southern parts of the study area. The spatial characteristics of urban land features on the 30m Landsat images were classified into five types: (1) agricultural land, (2) vegetation cover, (3) water bodies, (4) grassland, and (5) built-up areas. The classification was based on local knowledge of the area, the spectral responses of features in the Landsat images, the use of higher spatial resolution imagery, and visual analysis of different sensor data. Image classification was carried out using the supervised Random Forest (RF) classifier algorithm, which is widely applied in urban area analysis (Schneider, 2012), or using the Maximum Likelihood Classifier(Mahmon et al., 2015).

2.4 Urban Expansion Intensity Index (UEII)

Previously, several researchers have identified different measurement indices to characterize urban morphological changes based on remote sensing data by exploring the spatial and temporal dynamics of these indices. One such index, the Urban Expansion Intensity Index (UEII), is commonly used to measure and characterize growth in emerging urban areas over time (at least two relevant sources should be inserted). After extracting urban expansion from the Landsat images, we segmented the area into multiple concentric rings using concentric partitioning with the UEII (Equation 1) to quantitatively assess and analyze the differences in spatial expansion. The centers of the rings were placed at the town center (CBD), with intervals of 1.5 km between the rings. Although different studies have applied a maximum ring radius of 25 km, this study covered the entire municipal region within the selected area. The Urban Expansion Intensity Index for each ring was calculated using Equation 1. For example, Figure 2 shows the partitioned concentric rings used in the study area to characterize the spatial distribution of urban expansion, which is useful for urban planners and policymakers.

$$UEII = \frac{(UBA_{t+i} - UBA_t) x \frac{100}{i}}{SED} \quad \text{(Eqn 1)}$$

Were,
UEII: stand for the expansion intensity index of the urban built-up area in the spatial range between time (t) and $t + i$, UBA: stand for urban built-up area, and SED: represent the spatial expansion of the area.
After performing the UEII of the expansion of urban built-up area, we deploy a lognormal curve model (Eqn 2) in to fit the data of the city size distributions.

$$f(x) = \frac{a}{x\sigma\sqrt{2\pi}} x e^{\frac{(\ln x - \mu)^2}{2\sigma^2}}, \qquad x > 0. \qquad \text{(Eqn 2)}$$

Where, μ and σ are parameters of the shape of the fitted curve and a parameter a is represents its height. These parameters are defined as the optimal model.

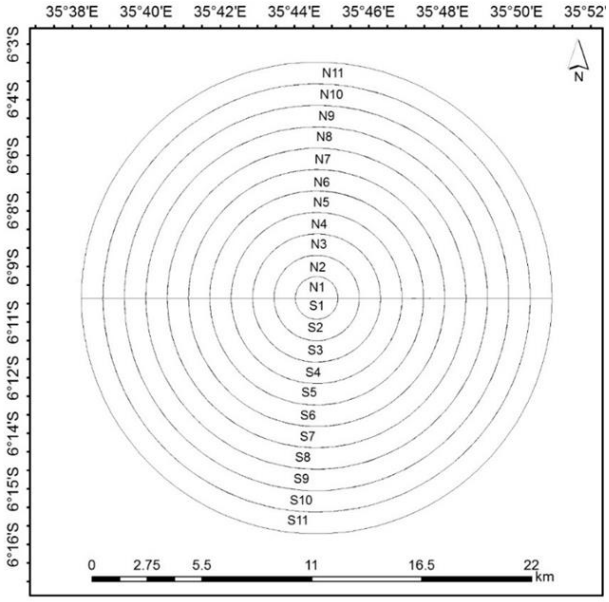

Figure 2: Partitioned concentric rings over the study area

Several characteristics metrics of urban growth model in Dodoma City Council were adopted in order to investigate the similarities and differences of its growth within the area.

2.5 Shannon's Entropy Index (SEI)

Shannon's Entropy method was further applied in this study to analyze urban growth based on the integration of remote sensing. The measurement of Entropy was derived based on factors (variables) distance from the city center, main roads and the fast point of development. The measurement is based on Entropy theory. In this study, Shannon's entropy (E) was used to measure the degree of spatial concentration by geographical factors (Thomas, 1981). Entropy is calculated by **Error! Reference source not found.**. Shannon's Entropy (SE) and Shannon's Relative Entropy (SRE) were performed on the northern and southern parts of the city of Dodoma using 0.5km buffer zones beginning from the city center from the year 1997 to 2018. In this research study, we considered different characteristics for instance patches size, shape and edge from the proposed landscape metrics and their description (Appendix 1) (Jat et al., 2008; Sumari et al., 2020).

Furthermore, Google Earth images acquired in 2019 were applied to verify the accuracy of the classified satellite images(Fu et al., 2019). The used to verify the accuracy of the classified results.

3. Results

3.1 Results of Urban Expansion Analysis in Dodoma

Figure 3 shows the map of urban extents from 1997 to 2018, where red area represents the new urban built-up land increase during 1997 to 2018. Landsat The analysis results show that urban built-up has extensively increased in the main roads, sub-towns and core area of the city center with the high impact of the transportation network on growth pattern (**Figure 4**)

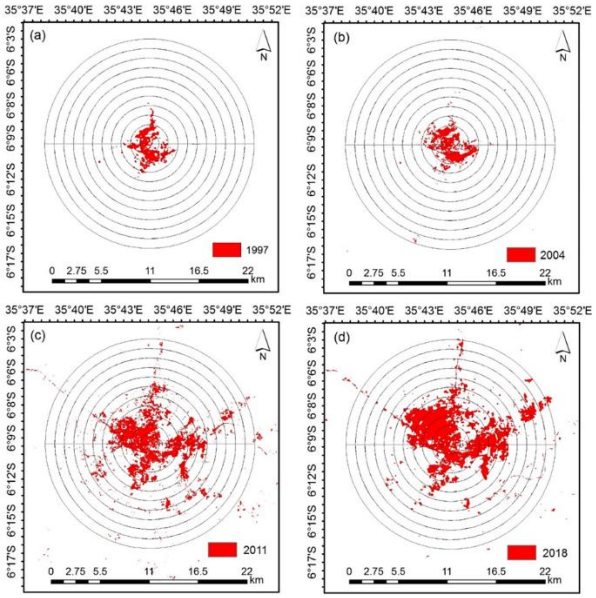

Figure 3: Urban area coverage and partitioned concentric rings for each year over the study area

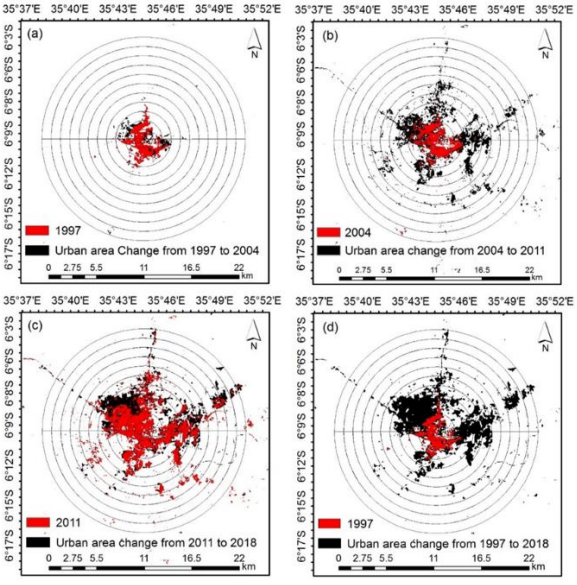

Figure 4: Urban area change and partitioned concentric rings over the study area

3.2 Characteristic Metrics of Urban Expansion

Figure 5 contains the log-normal fit (also known as Gaussian distribution) for the analyzed data of northern and southern sections of the city of Dodoma. The choice of this statistical test is based on its suitability for testing natural phenomena including changes in land use and land cover over time. The data on (**Error! Reference source not found.**) is positively skewed indicating that the distribution of land use and land cover data from the satellite images is log-normally distributed.

Table 1: UEII for North and South zones

	North Section	South Section
Sigma	1.7144	0.6228
FWHM	4.03711	1.46673
Height	0.30733	0.62131
R-square	0.7008	0.99045
a	1.32072	0.97005
Width	3.4288	0.09842
Peak position	4.533	4.51654
Skewness	1.020969	0.8793
Chi-square	0.00495	0.00031
F-value	18.23	329.56

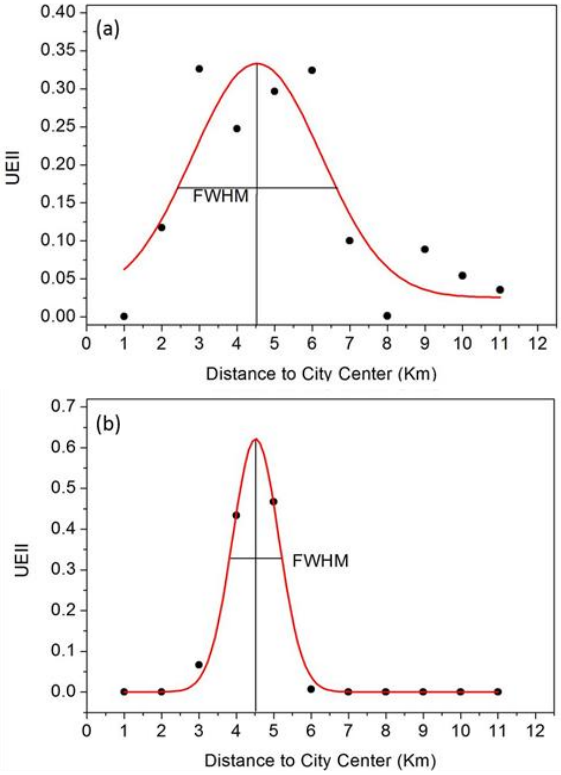

Figure 5: Lognormal curve of UEII and related metrics for (a) Northern and (b) Southern section of Dodoma

A quantitative expanse of urban growth of the city of Dodoma shows the different urban patterns, comparisons in zones, and changes identified within and between zones over the study epoch Figure 6. The amount of urban land was used mainly as a quantitative measure and as an indicator of urban expansion, and the pattern observed thereof. The urban built-up land was estimated for each classified zone for the 11 zones in the northern and southern sections of the study area as shown in Figure 5 above. The concentration of values of urban land shows that as at 2018, the N4, N5 and N3 ranked first, second and third in terms of expanse of urban built-up land use in the northern section of Dodoma while in the southern section, S3, S2 and S4 rank amongst the top 3 in the order of listing. The least urban land use coverage is found in N8 and S11 in north and south sections, respectively. A major similarity is in the corresponding increased/rapid growth in urban land use at N2, N3, N4, N5 and N6 (in the north section) and S2, S3, S4, S5, S6 (in the south section) parts of the city.

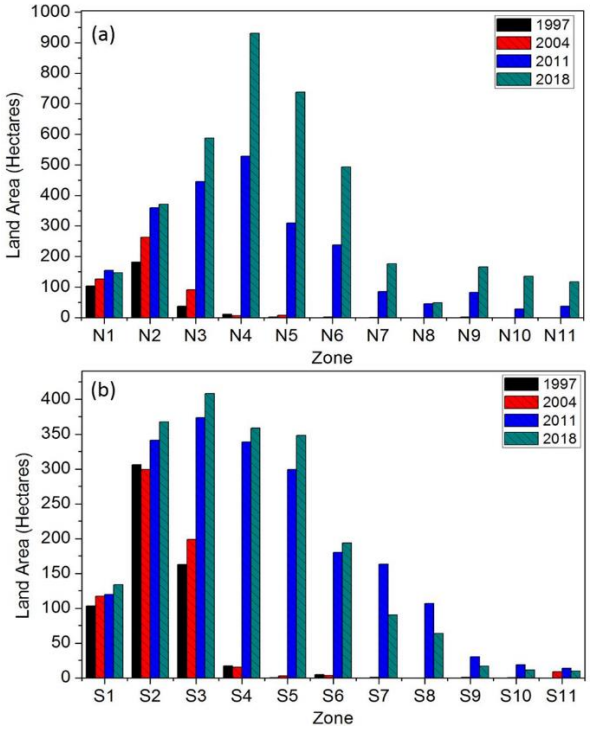

***Figure 6: Urban Land Area for the various zones for** (a) Northern and (b) Southern sections of the study area.*

2.3 Results of the Shannon's Entropy Index (SEI) analysis

The SEI results for the northern section of Dodoma show that the SE increased from 1997 (at 0.472179) to 2018 (at 0.911202), while the SRE value of 0.491724 in 1997 increased to 0.948919 in 2018. Given that the SE values range from 0 to 1, the 2018 SE and SRE values are quite high at 0.9 (**Error! Reference source not found.**). On the whole, the maximum values of SE and SRE are recorded in the northern zone. The pattern reveals consistent growth from 1997, 2004, 2011, and 2018 except for the year 2011 under the southern section where the SE and SRE are both higher than the values for the year 2018, revealing a disproportionate distribution between these two years in that section of the city.

Table 2: Shannon's Entropy and Relative Entropy

Year	Northern Section		Southern Section	
	Shannon's Entropy (SE)	Shannon's Relative Entropy (SRE)	Shannon's Entropy (SE)	Shannon's Relative Entropy (SRE)
2018	0.911202	0.948919	0.868307	0.904248
2011	0.896602	0.933715	0.910161	0.947835
2004	0.504486	0.525368	0.541075	0.563472
1997	0.472179	0.491724	0.497382	0.51797

The value of changes recorded in the SE between the study epochs across the northern and southern sections of Dodoma city is contained in **Error! Reference source not found.**. A negative trend is recorded from 2011-2018 in the southern section of the city. On the whole, the highest change is recorded in the northern section (0.439023) as against the recorded 0.370924 within the same study epoch but for the southern section. This suggests that the volume of data/information recorded over the former section is greater than the quantum recorded in the latter section of the city. This is a confirmation of (**Error! Reference source not found.**) where growth is revealed to be more expansive in the northern section of the city than the recorded growth for the southern part of the city between 1997 and 2018.

Within each zone, however, there is a disproportionate variation in changes recorded between study epochs. For example, the study epoch 2004 – 2011 in the northern zone records the highest changes of 0.408346 while the least change within the same zone is recorded in the study epoch 2011 – 2018. This is similar to the changes observed in the southern section of the city.

Table 3: Change in Shannon's Entropy

Year	Change in SE over Northern Zones	Change in SE over Southern Zones
2011 - 2018	0.015204	-0.04359
2004 - 2011	0.408346	0.384364
1997 - 2004	0.033644	0.045501
1997 - 2018	0.439023	0.370924

Sorensen's coefficient is defined as a similarity index indicator originally applied in Botanical studies to compare the similarities between two plant species and/or communities. **Error! Reference source not found.** reveals that the Sorensen's coefficient for this study records high values for two study epochs (1997 – 2004 at 0.680224 and 2011 – 2018 at 0.615461) implying that the similarity between the study years of these two study epochs is higher than not, given that the value of 1 indicates perfect similarity while 0 indicates perfect dissimilarity.

Table 4:Sorenson's coeff.

Year	Urban Land area (Ha)	Sorenson's coeff.
1997-2004	7894	0.680224041
2004-2011	11212	0.334073268
2011-2018	38590	0.615460678
2018 - 1997	9131	0.224103867

Table 5:Landscape Metrics

Parameter	1997	2004	2011	2018
AWMSI	4.1616	5.5168	7.1876	6.85341
MSI	1.3777	1.3267	1.3364	1.3221
MPAR	5679.1	12631.8	12795.5	7665.86
MPFD	1	1	1	1
AWMPFD	1	1	1	1
TE	0.713	1.3452	7.22131	4.66328
ED	1034.5	1601.42	2194.92	977.626
MPE	0.0155	0.005628	0.00432	0.00928
MPS	0.0000	3.51E-06	1.97E-0	9.5E-06
NumP	46	239	1671	502
MedPS	0	0	0	0
PSCoV	572.77	1323.637	2679.57	1738.93
PSSD	8.59E-05	4.65E-05	5.28E-05	0.00016
TLA	0.0006	0.00084	0.00329	0.00477
CA	0.0006	0.00084	0.00329	0.00477

Abbreviations: AWMSI: - Area-weighted mean shape index; MSI: - Mean shape index; MPAR: - Mean perimeter area ratio; MPFD: - Mean patch fractal dimension; AWMPFD: - Area weighted mean patch fractal dimension; TE: - Total edge; ED: - Edge density; MPE: - Mean patch edge; MPS: -Mean patch size; NumP: - Number of patches; MedPS: - Median patch size, PSCoV: - Patch size coefficient of variation; PSSD: - Patch size standard deviation; TLA: - Total area of the study area; CA: - Class Area

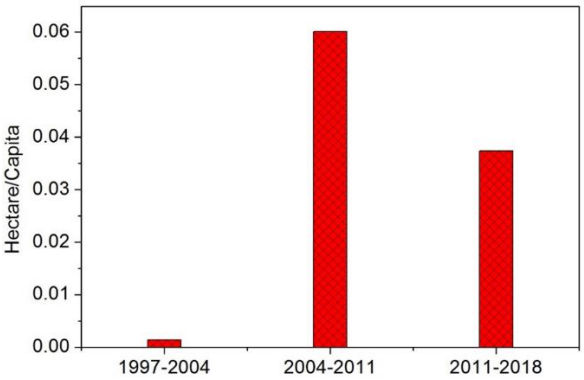

Figure 7: Land absorption

4. Discussion

The rapid expansion and population growth recorded in the Dodoma urban area have affected the ecosystems in the area both in terms of land degradation, water supply, loss of agricultural land, etc. This is because as growth increases, it exerts pressure on food, infrastructure and facilities (water, energy, roads, drainages, healthcare facilities, housing, etc.) and other natural resources, invariably translating into consumption of more natural resources as shown from the data analyses done for this study. In this regard, high population can lead to increased incidences of environmental degradation

especially where poverty is prevalent and where there is a lack of sufficient social services like waste management infrastructure and sanitation services, education, health, water, transport system and housing, implying a low quality of the population. The inability of Government authorities to adequately provide these critical infrastructures and facilities creates a vicious cycle of extreme poverty and low quality of life. It is therefore, extremely significant to control urban expansion as a prerequisite to a potentially sustainable socio-economic, environmental and urban management system.

The preliminary results of this study from satellite data analysis and in-situ field exercises suggest a rapid and expansion of Dodoma urban area, resulting in the loss of valuable agricultural land within and at the fringes of the city, thus affecting the source of livelihood of a significant population of the city that depend on agriculture as a major source of livelihood. In reality, critical infrastructure has not been able to keep-up with rapid urbanization and the lack of basic infrastructure and services can be easily observed in DUD such as water, sanitation, electricity, and waste management services. Regulatory agencies are yet to reticulate piped potable water to over half of the area and as a result most people rely on boreholes and hand-dug wells. Exacerbating the issue, the majority of these facilities are located outside the households forcing the population to travel sometimes 200m or even more to access water. Most residents of DUD dispose of their solid waste using a centralized collection container, but they sometimes have to travel as far as 300m to reach a solid waste collection point. This has led to some residents to dump their waste in unauthorized collection points. This coupled with the lack of drainage facilities has led to annual urban floods, while liquid waste is dumped in the open creating sanitation challenges. It would appear as if planning for the expanding fringes in DUD is not done prior to development. This trend needs to be reversed to institute a sustainable urban planning system for DUD.

5. Conclusions

The result of the case study has demonstrated that the Federal Capital City of Dodoma Urban is experiencing rapid growth by considering several approaches including Geospatial information Science (GIS) and Remote Sensing (RS). This article underwrites to the prevailing works on Spatiotemporal analysis of urban expansion with remote sensing studies with various perceptions. This expansion and population growth recorded in the Dodoma Urban District area have led into the effect-side for the ecosystems for various aspects of either land degradation, water supply, loss of agricultural land, which have been due to the increase in the population growth of an area. In this regard, the high population can lead to increased incidences of environmental degradation especially where poverty is prevalent and where there is a lack of sufficient social services like waste management infrastructure and sanitation services, education, health, water, transport system, and housing, implying a low quality of the population. However, the results of the study from the satellite datum analysis and various field exercises have suggested a rapid seemingly uncontrolled expansion of Dodoma's urban area, resulting in the loss of valuable agricultural land within and at the fringes of the city, thus affecting the source of livelihood of a significant population of the city that depend on agriculture as a major source of livelihood. In built-up areas with a SEI of 0.439023 (northern region) and 0.370924 (Southern region) between 1997 and 2018. The image classification can be used to provide accurate land use and land cover change maps and predict future changes. The urban expansion analysis results investigated the extensive increase in the built-up which is in the main roads and the other core places of the center that have more impacts on the transportation network for the growth pattern. Moreover, the increased urbanization concentration in Tanzania specifically in the Dodoma region has created several socioeconomic, policy, and environmental factors as the drivers that stem from extensive urban poverty, recurrent flooding, slum growth, extensive alteration of wetland ecosystems, and mismanagement of limited resources.

References

Addaney, M., & Cobbinah, P. B. (2019). Climate Change, Urban Planning and Sustainable Development in Africa: The Difference Worth Appreciating. In *The Geography of Climate Change Adaptation in Urban Africa*. Springer International Publishing. https://doi.org/10.1007/978-3-030-04873-0_1

Bonafoni, S., & Keeratikasikorn, C. (2018). Land surface temperature and urban density: Multiyear modeling and relationship analysis using modis and landsat data. *Remote Sensing*, *10*(9). https://doi.org/10.3390/rs10091471

Brusseau, M. L. (2019). Ecosystems and Ecosystem Services. In *Environmental and Pollution Science* (3rd ed.). Elsevier Inc. https://doi.org/10.1016/b978-0-12-814719-1.00006-9

Chove, L. H., & Sumari, N. S. (2025). *In What Ways Do Road Networks Influence the Spatial Characteristics of Urban Expansion ? A Case Study of Morogoro Municipality*. 26–27.

Cobbinah, P. B. (2015). Local attitudes towards natural resources management in rural Ghana. *Management of Environmental Quality: An International Journal*, *26*(3), 423–436. https://doi.org/10.1108/MEQ-04-2014-0061

Cobbinah, P. B., & Darkwah, R. M. (2017). Toward a more desirable form of sustainable urban development in Africa. *African Geographical Review*, *36*(3), 262–285. https://doi.org/10.1080/19376812.2016.1208770

Fu, H., Shao, Z., Fu, P., & Cheng, Q. (2017). The dynamic analysis between urban nighttime economy and urbanization using the DMSP/OLS nighttime light data in China from 1992 to 2012. *Remote Sensing*, *9*(5). https://doi.org/10.3390/rs9050416

Fu, Y., Li, J., Weng, Q., Zheng, Q., Li, L., Dai, S., & Guo, B. (2019). Characterizing the spatial pattern of annual

urban growth by using time series Landsat imagery. *Science of the Total Environment*, *666*(February), 274–284. https://doi.org/10.1016/j.scitotenv.2019.02.178

Gombe, K. E., Asanuma, I., & Park, J.-G. (2017). Quantification of Annual Urban Growth of Dar es Salaam Tanzania from Landsat Time Series Data. *Advances in Remote Sensing*, *06*(03), 175–191. https://doi.org/10.4236/ars.2017.63013

Guastella, G., Oueslati, W., & Pareglio, S. (2019). Patterns of urban spatial expansion in European Cities. *Sustainability (Switzerland)*, *11*(8), 1–15. https://doi.org/10.3390/su11082247

Jat, M. K., Garg, P. K., & Khare, D. (2008). Monitoring and modelling of urban sprawl using remote sensing and GIS techniques. *International Journal of Applied Earth Observation and Geoinformation*, *10*(1), 26–43. https://doi.org/10.1016/j.jag.2007.04.002

Jia, T., Chen, K., & Wang, J. (2017). Characterizing the growth patterns of 45 major metropolitans in Mainland China using DMSP/OLS data. *Remote Sensing*, *9*(6). https://doi.org/10.3390/rs9060571

Jiao, L., Dong, T., Xu, G., Zhou, Z., Liu, J., & Liu, Y. (2021). Geographic micro-process model: Understanding global urban expansion from a process-oriented view. *Computers, Environment and Urban Systems*, *87*(May), 101603. https://doi.org/10.1016/j.compenvurbsys.2021.101603

Kabanda, T. (2019). Land use/cover changes and prediction of Dodoma, Tanzania. *African Journal of Science, Technology, Innovation and Development*, *11*(1), 55–60. https://doi.org/10.1080/20421338.2018.1550925

Kisamba, F. C., & Li, F. (2023). Analysis and modelling urban growth of Dodoma urban district in Tanzania using an integrated CA–Markov model. *GeoJournal*, *88*(1), 511–532. https://doi.org/10.1007/s10708-022-10617-4

Kontgis, C., Schneider, A., Fox, J., Saksena, S., Spencer, J. H., & Castrence, M. (2014). Monitoring peri-urbanization in the greater Ho Chi Minh City metropolitan area. *Applied Geography*, *53*, 377–388. https://doi.org/10.1016/j.apgeog.2014.06.029

Korah, P. I., & Cobbinah, P. B. (2017). Juggling through ghanaian urbanisation: Flood hazard mapping of kumasi. *GeoJournal*, *82*(6), 1195–1212. https://doi.org/10.1007/s10708-016-9746-7

Kuffer, M., Wang, J., Nagenborg, M., Pfeffer, K., Kohli, D., Sliuzas, R., & Persello, C. (2018). The scope of earth-observation to improve the consistency of the SDG slum indicator. *ISPRS International Journal of Geo-Information*, *7*(11), 1–28. https://doi.org/10.3390/ijgi7110428

Lai, J., Zhan, W., Huang, F., Voogt, J., Bechtel, B., Allen, M., Peng, S., Hong, F., Liu, Y., & Du, P. (2018). Identification of typical diurnal patterns for clear-sky climatology of surface urban heat islands. *Remote Sensing of Environment*, *217*(July), 203–220. https://doi.org/10.1016/j.rse.2018.08.021

Lu, M., Chen, J., Tang, H., Rao, Y., Yang, P., & Wu, W. (2016). Land cover change detection by integrating object-based data blending model of Landsat and MODIS. *Remote Sensing of Environment*, *184*, 374–386. https://doi.org/10.1016/j.rse.2016.07.028

Mahmon, N. A., Ya’Acob, N., & Yusof, A. L. (2015). Differences of image classification techniques for land use and land cover classification. *Proceedings - 2015 IEEE 11th International Colloquium on Signal Processing and Its Applications, CSPA 2015*, 90–94. https://doi.org/10.1109/CSPA.2015.7225624

Meng, Q., Zhang, L., Sun, Z., Meng, F., Wang, L., & Sun, Y. (2018). Characterizing spatial and temporal trends of surface urban heat island effect in an urban main built-up area: A 12-year case study in Beijing, China. *Remote Sensing of Environment*, *204*(September 2017), 826–837. https://doi.org/10.1016/j.rse.2017.09.019

Mundia, C. N., & Murayama, Y. (2009). Analysis of land use/cover changes and animal population dynamics in a wildlife sanctuary in East Africa. *Remote Sensing*, *1*(4), 952–970. https://doi.org/10.3390/rs1040952

Mwampamba, T. H. (2007). Has the woodfuel crisis returned? Urban charcoal consumption in Tanzania and its implications to present and future forest availability. *Energy Policy*, *35*(8), 4221–4234. https://doi.org/10.1016/j.enpol.2007.02.010

Pandey, B., & Seto, K. C. (2015). Urbanization and agricultural land loss in India: Comparing satellite estimates with census data. *Journal of Environmental Management*, *148*, 53–66. https://doi.org/10.1016/j.jenvman.2014.05.014

Qin, Y., Xiao, X., Dong, J., Chen, B., Liu, F., Zhang, G., Zhang, Y., Wang, J., & Wu, X. (2017). Quantifying annual changes in built-up area in complex urban-rural landscapes from analyses of PALSAR and Landsat images. *ISPRS Journal of Photogrammetry and Remote Sensing*, *124*, 89–105. https://doi.org/10.1016/j.isprsjprs.2016.12.011

Ringo, J. (2016). Status of Sewage Disposal in Dodoma Municipality, Tanzania. *International Journal of Marine, Atmospheric & Earth Sciences Int. J. Mar. Atmos. & Earth Sci*, *4*(1), 24–34. www.ModernScientificPress.com/Journals/IJMaes.aspx

Schneider, A. (2012). Monitoring land cover change in urban and peri-urban areas using dense time stacks of Landsat satellite data and a data mining approach. *Remote Sensing of Environment*, *124*, 689–704. https://doi.org/10.1016/j.rse.2012.06.006

Shao, Z., Sumari, N. S., Portnov, A., Ujoh, F., Musakwa, W., & Mandela, P. J. (2021). Urban sprawl and its impact on sustainable urban development: a combination of

remote sensing and social media data. *Geo-Spatial Information Science*, *24*(2), 241–255. https://doi.org/10.1080/10095020.2020.1787800

Sumari, N. S., Cobbinah, P. B., Ujoh, F., & Xu, G. (2020). On the absurdity of rapid urbanization: Spatio-temporal analysis of land-use changes in Morogoro, Tanzania. *Cities*, *107*(June), 102876. https://doi.org/10.1016/j.cities.2020.102876

Terfa, B. K., Chen, N., Liu, D., Zhang, X., & Niyogi, D. (2019). Urban expansion in Ethiopia from 1987 to 2017: Characteristics, spatial patterns, and driving forces. *Sustainability (Switzerland)*, *11*(10), 1–21. https://doi.org/10.3390/su11102973

Thomas, R. W. (1981). Information statistics in geography. In *Information statistics in geography.* Geo Abstracts.

URT. (2018). *National Population Projections, Feb 2018*.

Wang, Z. H., & Upreti, R. (2019). A scenario analysis of thermal environmental changes induced by urban growth in Colorado River Basin, USA. *Landscape and Urban Planning*, *181*, 125–138. https://doi.org/10.1016/j.landurbplan.2018.10.002

Worrall, L., Colenbrander, S., Palmer, I., Makene, F., Mushi, D., Kida, T., Martine, M., & Godfrey, N. (2017). Better Urban Growth in Tanzania: A Preliminary Exploration of the Opportunties and Challenges. In *Coalition for Urban Transitions*. http://www.esrf.or.tz/docs/NCE2017_Better_Urban_Growth_Tanzania_final.pdf

Wu, S., Sumari, N. S., Dong, T., Xu, G., & Liu, Y. (2021). Characterizing Urban Expansion Combining Concentric-Ring and Grid-Based Analysis for Latin American Cities. *Land*. https://doi.org/https://doi.org/10.3390/land10050444

Xiao, R., Murayama, Y., Qin, K., Su, J., Gao, Z., Liu, L., Xu, G., & Jiao, L. (2024). Urban expansion in highly populous East Asian megacities during 1990–2020: Tokyo, Seoul, Beijing, and Shanghai. *Ecological Informatics*, *83*(October), 102843. https://doi.org/10.1016/j.ecoinf.2024.102843

Xiong, Y., Huang, S., Chen, F., Ye, H., Wang, C., & Zhu, C. (2012). The Impacts of Rapid Urbanization on the Thermal Environment: A Remote Sensing Study of Guangzhou, South China. *Remote Sensing*, *4*(7), 2033–2056. https://doi.org/10.3390/rs4072033

Xu, G., Dong, T., Cobbinah, P. B., Jiao, L., Sumari, N. S., Chai, B., & Liu, Y. (2019). Urban expansion and form changes across African cities with a global outlook: Spatiotemporal analysis of urban land densities. *Journal of Cleaner Production*, *224*, 802–810. https://doi.org/10.1016/j.jclepro.2019.03.276

Xu, G., Jiao, L., Liu, J., Shi, Z., Zeng, C., & Liu, Y. (2019). Understanding urban expansion combining macro patterns and micro dynamics in three Southeast Asian megacities. *Science of the Total Environment*, *660*(41771429), 375–383. https://doi.org/10.1016/j.scitotenv.2019.01.039

Xu, G., Zhou, Z., Jiao, L., Dong, T., & Li, R. (2019). Cross-sectional urban scaling fails in predicting temporal growth of cities. *ArXiv*. http://arxiv.org/abs/1910.06732

Yang, J., Pan, S., Dangal, S., Zhang, B., Wang, S., & Tian, H. (2017). Continental-scale quantification of post-fire vegetation greenness recovery in temperate and boreal North America. *Remote Sensing of Environment*, *199*(July), 277–290. https://doi.org/10.1016/j.rse.2017.07.022

Yang, J., Wu, T., & Gong, P. (2017). Implementation of China’s new urbanization strategy requires new thinking. *Science Bulletin*, *62*(2), 81–82. https://doi.org/10.1016/j.scib.2016.12.013

Appendix 1: Proposed Landscape metrics used in this study

	Equations	Range: unit	Interpretation
Patch density and size	$\mathbf{CA} = \sum_{j=1}^{n} a_{ij} \left(\frac{1}{10{,}000}\right)$	>0; ha	As patch type becoming rare, Class area (CA) methods 0. CA = TA when single patch forms the landscape.
	$\boldsymbol{NP} = ni$	≥	Number of patches= 1 when single patch forms the landscape
	$\boldsymbol{PD} = \frac{ni}{A}(10{,}000)(100)$	>0; no/ 100 ha	Higher value of patch density (PD) indicates more fragmentation of urban landscape
	$MedPS = X_{50\%}$	50th %; ha	Median patch size is the middle patch size in the distribution
	$\boldsymbol{PSSD} = \sqrt{\frac{\sum_{j=1}^{n}[a_{ij} - (\frac{\sum_{j=1}^{n} a_{ij}}{ni})]}{ni}} \left(\frac{1}{10{,}000}\right)$	≥0; ha	Patch size standard deviation (PSSD)=0 when there is no variability in patch size or when where is on patch. The value increases with area variability among patches
	$PScoV = \frac{PSSD}{MPS}(100)$	≥0; %	It is coefficient of variability in patch size relative to the mean patch size. PScoV increases as the variability increases
	$MPS = \frac{\sum_{j=1}^{n} a_{ij}}{ni}\left(\frac{1}{10{,}000}\right)$	>0; ha	It is the average patch size
	$LPI = \frac{j=1}{A}(100)$	0<LPI≤100; %	Largest patch index (LPI) quantifies patch dominance. The value near zero indicates smaller largest patch. LPI = 100 when sing patch creates the landscape.
Shape	$AWMSI = \sum_{j=i}^{n}[(\frac{p_{ij}}{\sqrt[2]{\pi * a_{ij}}})(\frac{a_{ij}}{\sum_{j=1}^{n} a_{ij}})]$	≥1; no unit	It is average shape index of patches weighted by patch area so that larger patches weigh more than smaller patches. AWMSI=1, indicates all patches are circular (vector), whereas the value increases with shape irregularity
	$MSI = \frac{\sum_{j=i}^{n}(\frac{p_{ij}}{\sqrt[2]{\pi * a_{ij}}})}{ni}$	≥1; no unit	MSI=1 when all patches of the corresponding patches types are circular (vector) and it increases with irregularity of shape
	$MPAR = \frac{\sum_{j=1}^{n} \frac{p_{ij}}{a_{ij}}}{ni}$	>0; no unit	MPAR measures average shape complexity. The higher the value, the more irregularity of the patches’ shape
	$MPFD = \frac{\sum_{j=1}^{n} \frac{2lnp_{ij}}{lna_{ij}}}{ni}$	[1-2] no unit	MPFD approaches to 2, implies the departure from Euclidean geometry (shape with highly convoluted) and vice versa.
	$AWMPFD = \sum_{j=i}^{n}[(\frac{2lnp_{ij}}{lna_{ij}})(\frac{a_{ij}}{\sum_{j=1}^{n} a_{ij}})]$	[-2] no unit	AWMPFD approach to 2 implies departure from Euclidean geometry (increasing shape complexity) and it approaches 1 for very simple perimeters (circle)
Edge	$TE = \sum_{k=1}^{m'} e_{ik}$	≥0; M	Total edge (TE)=0 means no class edge (consists single patch) or none of the landscape boundary and background edge be treated as edge. It measures how dissected spatial pattern is
	$MPE = {}^{TE}/_{ni}$		MPE is mean patch edge

For $j = 1,\ldots, n$ patches and; $k = 1,\ldots, m$ or m patch. Symbols MPFD, mean patch fractal dimension; AWMPFD, area-weighted mean patch fractal dimension; *ni*, number of patches in the landscape of patch *i*; a_{ij}, the area of patch *ij* in the class; A, total landscape area (m2); pij , perimeter (m) of patch *ij*; M_{max}, the maximum; *ln*, natural logarithm; e_{ik}, total length (m) of edge in landscape between patch *i* and *k* which includes landscape boundary segments representing true edge only involving patch type *i*; *m* , number of patch present in the landscape including the landscape border if present